

# Toward Understanding of Bio-Oil Aging: Accelerated Aging of Bio-Oil Fractions

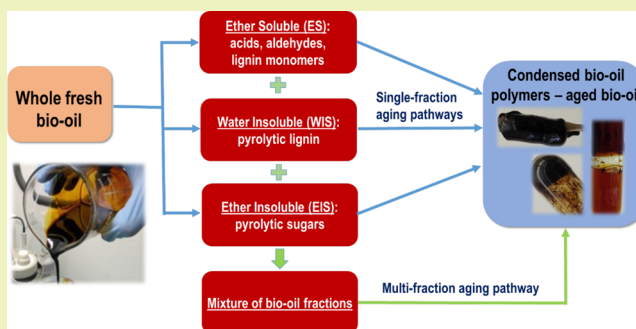
Jiajia Meng, Andrew Moore, David Tilotta, Stephen Kelley, and Sunkyu Park\*

Department of Forest Biomaterials, North Carolina State University, Raleigh, North Carolina 27695, United States

## Supporting Information

**ABSTRACT:** Pyrolysis bio-oil from biomass is a promising intermediate for producing transportation fuels and platform chemicals. However, its instability, often called aging, has been identified as a critical hurdle that prevents bio-oil from being commercialized. The objective of this research is to explore the bio-oil aging mechanism by an accelerated aging test of fractionated bio-oil produced from loblolly pine. When water soluble (WS), ether insoluble (EIS), and pyrolytic lignin (PL) fractions were aged separately, the increased molecular weight (Mw) was observed with increasing aging temperature and the presence of acids. WS and EIS fractions had high Mw brown solids formed after aging. Adjusting the pH of WS and EIS fractions from 2.5 to 7.0 significantly reduced the tendency of a Mw increase. Similar Mw rise was also observed on a PL fraction with an elevated temperature and acid addition. Formaldehyde was found to react with the PL fraction in the presence of any acid catalysts tested, i.e., 8-fold Mw increase in acetic acid environment, while other bio-oil aldehydes did not significantly promote lignin condensation. To better understand bio-oil stability, a potential bio-oil aging pattern was proposed, suggesting that bio-oil can be aged within or between its fractions.

**KEYWORDS:** Bio-oil, Aging, Stability, Fast pyrolysis, Pyrolytic lignin



## INTRODUCTION

Bio-oil condensed from biomass pyrolysis vapor is a dark-brown viscous liquid and has economic potential to be upgraded into transportation fuels using current refinery infrastructure. However, it shares no similarities with fossil oil in terms of fuel property. Typical bio-oil contains high oxygen, water, and acid content. Due to the presence of oxygen-rich compounds, e.g. aldehydes, bio-oil is neither chemically nor thermally stable. The unstable nature of pyrolysis oil makes its storage and further upgrading challenging, as aged bio-oil typically shows increased water content, viscosity, and phase separation. In addition, catalyst coke formation is also closely related to its high reactivity during upgrading at an elevated temperature.<sup>1</sup>

The bio-oil aging phenomena can be explained by polymerization of bio-oil components under acidic and thermal conditions catalyzed by the mineral compounds contained in bio-oil char particles.<sup>2,3</sup> Diebold<sup>4</sup> proposed that diverse aging reactions could occur in bio-oil, e.g., esterification of organic acids with alcohols and resin formation from aldehydes and phenols. However, none of these proposed reactions have been experimentally verified in a chemical environment similar to bio-oil. Therefore, the current knowledge on bio-oil aging and its reaction chemistry is largely based on empirical correlation and speculations.

The extreme complexity of bio-oil composition adds great difficulties to its aging mechanism study. Current aging research

mainly focuses on developing strategies to slow down its aging rate based on observations of the physicochemical changes in bulky bio-oil properties.<sup>5–8</sup> Studies on bio-oil polymerization at a molecular level have rarely been published because the result interpretation is nearly impossible with over 300 different chemical compounds in bio-oil. Hu and his co-workers<sup>9</sup> reported a bio-oil polymerization study by heating the bio-oil model compounds under gradually increased temperature and concluded that sugars, acids, phenolics, and furans contribute significantly to bio-oil instability. Although this work is of great importance to the understanding of bio-oil aging reactions, the model compounds used in the study did not represent the whole bio-oil composition.

An ideal substrate for an aging study that can be representative but also has relatively simple composition is a fractionated bio-oil. Additionally, the heterogeneous nature of bio-oil as a microemulsion<sup>10</sup> might suggest that the actual aging reaction could preferentially occur in each individual fraction. Therefore, the aging study using an individual bio-oil fraction and its mixture is expected to provide an insight on aging mechanisms.

A bio-oil fractionation has been developed<sup>11</sup> by water extraction to separate bio-oil into a water soluble (WS) and

Received: March 31, 2014

Revised: July 4, 2014

Published: July 11, 2014

water insoluble fraction (WIS); the water soluble fraction can be further extracted with diethyl ether and fractionated into an ether soluble (ES) and ether insoluble (EIS) fraction. The water insoluble fraction is typically referred to as pyrolytic lignin that contains lignin monomers, e.g., guaiacol and oligomers. The ether insoluble fraction is defined as pyrolytic sugar that contains anhydrosugars, oligo/polysaccharides, and aliphatic hydroxyacids. The ether soluble fraction contains mainly volatile organics, such as aldehydes, ketones, alcohols, and acids. Applying these fractions into a bio-oil aging study can help elucidate their individual role in bio-oil reaction chemistry.

In this work, an investigation on the bio-oil aging reactions under different temperature and pH has been performed on isolated bio-oil fractions, which are much more representative to actual reaction environments than model compounds. This particular aging study, for the first time, demonstrated the aging behavior of individual bio-oil fractions. Additionally, one of the most probable aging interactions between aldehydes and pyrolytic lignin was carried out with various aldehyde compounds identified in bio-oil.

## EXPERIMENTAL SECTION

**Bio-Oil Production.** Loblolly pine chips were ground and sieved into small particles (<0.5 mm). The bio-oil was produced using a fluidized bed reactor (O.D. 43 mm, 150 g/h feed capacity) at  $500 \pm 10$  °C with ~1 s residence time as described previously.<sup>12</sup> A total of 1 L of raw bio-oil was produced for the aging study with an average liquid yield of ~65%. The elemental analysis and physicochemical properties of fresh and aged bio-oil such as water content, viscosity, molecular weight, and TAN (total acid number) are summarized in Table 1.

**Table 1. Characterization of Fresh and Accelerated Aged Bio-Oil from Loblolly Pine**

	raw bio-oil	aged bio-oil <sup>a</sup>
<b>elemental analysis (dry base)</b>		
C, %	50.1	51.1
H, %	6.65	6.31
O, % <sup>b</sup>	42.7	42.0
N, %	0.53	0.63
O/C atomic ratio	0.64	0.62
<b>physicochemical properties</b>		
water content, %	19.8	23.9
viscosity, cp	16.4	55.7
Mw <sup>c</sup> , g/mol	340	660
Mn <sup>c</sup> , g/mol	270	370
TAN, mg KOH/g	58.9	68.5

<sup>a</sup>Accelerated aged at 80 °C for 24 h. <sup>b</sup>Oxygen content was calculated by difference. <sup>c</sup>Mw and Mn are determined by a RI detector.

**Solvent Fractionation.** The bio-oil solvent fractionation was performed according to a method described elsewhere.<sup>13</sup> Simply, the bio-oil was first extracted with excess DI water (bio-oil:water = 1:30 wt ratio) and separated into water soluble (WS) and water insoluble (WIS) fractions. The WS fraction was further extracted with diethyl ether (v:v = 1:1) into ether soluble (ES) and ether insoluble (EIS) fractions. The WIS fraction was extracted with dichloromethane (v:v = 1:1) into low molecular mass lignin (LMM) and high molecular mass (HMM) lignin fractions.

**Bio-Oil Accelerated Aging.** Approximately 10 g of bio-oil was aged in a reaction tube (ACE 8648-04) under 80 °C for 24 h in a convection oven.<sup>14</sup> The bio-oil aging index was calculated according to eq 1, where P stands for a particular bio-oil property. Accelerated aging is denoted as AA.

$$\text{Aging index} = \frac{(P_{\text{Aged bio-oil}} - P_{\text{Initial bio-oil}})}{P_{\text{Initial bio-oil}}} \times 100\% \quad (1)$$

For the accelerated aging of bio-oil fractions, 10 g of bio-oil WS fraction (~90% water, pH 2.5) and EIS sugar fraction (~80% water, pH 2.6) were aged under 80 and 110 °C, respectively, for 24 h. To investigate the pH effect on bio-oil aging severity, WS and EIS fractions were neutralized using NaOH and aged at 80 °C. The aged WS fractions were dissolved in THF for GPC (gel permeation chromatography) analyses, and the aged EIS fraction were rotary vacuum-dried for further <sup>13</sup>C NMR and GPC characterization. Accelerated aging of the WIS lignin fraction (~3% water, 1g loading) was performed with/without adding carboxylic acids (acetic and formic acids) under 80 or 110 °C for 24 h. The aged lignin samples were rotary vacuum-dried to remove the moisture and acids for further GPC and <sup>13</sup>C NMR characterization. The aging experiments were repeated at least twice, and the average value was reported.

**Bio-Oil Characterization: GPC and NMR.** The average molecular weight was analyzed by GPC (Shimadzu HPLC, LC-20AD) with a RI and an UV detector. Two columns (Waters, HR-1 and HR-5E) at 35 °C were connected for the separation of bio-oil components. Tetrahydrofuran (THF) was used as the mobile phase at 0.7 mL/min. The samples were dissolved in THF to approximately 0.5 mg/mL (pyrolytic lignin) or 2 mg/mL (others) and then filtered through a 0.25 μm filter. Twelve polystyrene standards with the molecular weight ranging from 162 to 3,520,000 g/mol were used to generate a calibration curve.

<sup>13</sup>C NMR characterization of bio-oils was recorded in a DMSO-*d*<sub>6</sub> solution (25% wt/wt) with a 5 mm NMR tube using a Bruker Avance 700 MHz NMR spectrometer. The NMR experiments were conducted with a cryoprobe (279 K). <sup>13</sup>C spectrum was obtained by an inverse gated decoupling pulse sequence, 90° pulse angle, 2.5 s pulse delay time, and a total of ~20,000 scans at 25 °C. The spectra integration was conducted using Topspin 3.2.

**Phenol–Glycolaldehyde Reaction.** Glycolaldehyde was generated in situ when heating the glycolaldehyde dimmer (Sigma-Aldrich, G6805) solution above 70 °C during the reaction.<sup>15</sup> In three vials, 0.01 mol of phenol and 0.005 mol of glycolaldehyde dimer was prepared along with three different acid catalysts: (a) 3 mL of acetic acid, (b) 3 mL of formic acid, and (c) 3 mL of HCl (0.5 mol/mL). One milliliter of DI water was added into the reaction vials when acetic acid and formic acid were used. A control vial with 0.005 mol of glycolaldehyde dimer and 3 mL of HCl (0.5 mol/mL) without phenol addition was also included. After mixing, the four vials were placed in a silicone oil bath at 90 °C for 24, 12, 5, and 2 h, respectively. The reaction products were rotary vacuum-dried to remove the water and acids for <sup>13</sup>C NMR characterization.

**Pyrolytic Lignin–Aldehydes Reaction.** Approximately 60 g of pyrolytic lignin (PL) was isolated from bio-oil using the ice–water precipitation method.<sup>16</sup> The collected wet lignin was vacuum-dried at 30 °C for 24 h. After vacuum drying, PL was in a sticky gum shape, similar to plasticene, and contained ~3% moisture.

Several aldehydes identified in bio-oil, including formaldehyde,<sup>17</sup> glycolaldehyde, furfural, hydroxymethylfurfural (HMF), and vanillin, were reacted with PL under 80 °C for 24 h. Approximately, 1 g of PL along with the aldehydes and acid catalyst were added into a 15 mL reaction tube. The weight ratio between PL to aldehydes and acid was kept at 6:1:6. In addition, 0.3 mL of DI water was added into the reaction tubes except the one containing formaldehyde, as formaldehyde was already added as a water solution (37 wt %). The carboxylic acids could fully dissolve the lignin, forming a uniform reaction media for the potential reaction between PL and aldehydes. After the reaction, the solutions were cooled to room temperature and vacuum-dried. In the case of the solid resin formed in the reaction tube, the reaction products were dissolved in acetone and then vacuum-dried. <sup>13</sup>C NMR analyses of the lignin–aldehyde reaction products were conducted with a Bruker Avance DRX 500 MHz NMR spectrometer.

## RESULTS AND DISCUSSION

**Individual Aging of Bio-Oil Fractions.** *Accelerated Aging of Water Soluble Fraction and Ether Insoluble Sugar Fraction.* It has been suggested that the aldehydes, acids, and sugars are the main villains causing bio-oil aging and catalyst coking,<sup>4,18–20</sup> and the WS fraction is the main host of these three groups. Therefore, understanding the aging behavior of the WS fraction is critical to reveal the overall bio-oil aging mechanism. In addition, as part of the WS fraction, the EIS sugar fraction also participates actively in the aging reactions, as these sugars are typically reactive under acidic heating conditions.

The initial WS and EIS fractions were light-yellow clear liquids. After accelerated aging at 80 °C, there was a trace amount of brown solids formed, but the liquid color of the aged WS and EIS remained unchanged. When aged at 110 °C, a significant amount of dark-brown solids (arrows in Figure 1),

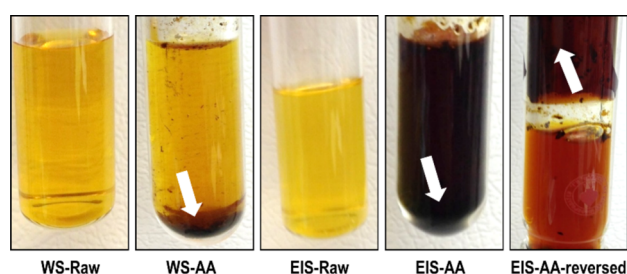


**Figure 1.** Visual appearance of bio-oil WS (water soluble) and EIS (ether insoluble) fractions after accelerated aging at 110 °C. Arrow indicates solids formed. A layer of solids adhered to the tube wall in the EIS-AA were observed by reversing the reaction tube (EIS-AA-reversed).

especially for the EIS fraction (~0.30% for WS and ~1.25% for EIS based on dry WS and EIS fractions), was accumulated inside the tube. The solid formation from the aged WS and EIS fractions explains why they had a decreased quantity observed from the results on the whole bio-oil aging. The average molecular weight of accelerated aged bio-oil fractions are summarized in Table S1 of the Supporting Information, and the Mw aging indexes are plotted in Figure 2. After a heat treatment under an acidic condition (pH 2.5) at 80 °C, no apparent Mw change was observed for the liquid phase of the aged WS and EIS fractions (Figure 2a). However, the precipitated brown solids showed a significant Mw increase

when compared to their starting liquid fractions. Similar but more pronounced effects, especially for the WS fraction, have been found when the aging temperature was adjusted to 110 °C.

The detailed aging mechanism of the WS and EIS fractions is not clearly demonstrated in the literature, but it is considered to be initiated by acid-catalyzed sugar decomposition forming reactive compounds such as hydroxymethylfurfural, which possess hydroxyl, carbonyl groups, and conjugated double bonds, followed by repolymerization of these degradation products (Figure 3a). In this reaction pathway, the acid catalyst plays an important role in promoting the initial sugar degradation and the secondary repolymerization reactions. Therefore, it is expected that the reaction rate would be significantly decreased if the acids could be removed from the bio-oil fractions. To test this hypothesis, the pH value of the WS and EIS fractions was slowly adjusted to 7.0, and the resulting neutral fractions were aged under 80 °C for 24 h. After aging, the WS and EIS fractions, especially the solid parts, showed a significantly less molecular weight increase than that under acidic conditions in Figure 2b. Similar results were also observed when whole bio-oils were neutralized and aged under accelerated aging conditions. This suggests that the condensation reactions of WS and EIS fractions are acid-catalyzed reactions.

To further elucidate the aging reaction of pyrolytic sugar, the fresh and aged EIS fractions were analyzed by <sup>13</sup>C NMR. In Table 2, the carbonyl carbon decreased, while the amount of C=C carbon increased significantly after aging. The reduced carbonyl signal could be achieved by condensation reactions similar to aldol condensation in Figure 3b. The increased C=C carbon may support the above-mentioned sugar degradation and repolymerization path as the typical sugar degradation products, e.g., furfural, contain such conjugated carbon double bonds. In addition, the aldol condensation products also contain such  $\pi$  bonds. For the six carbon sugar ring structure, the number of C<sub>1</sub> end carbons and C<sub>1</sub>–O–C<sub>4</sub> carbons decreased, while the aliphatic carbons increased. The content of C<sub>2,3,4,5,6</sub> carbons remain unchanged. The reduced C<sub>1</sub> end carbon and C<sub>1</sub>–O–C<sub>4</sub> carbon suggests that the sugar fragmentation may occur at a sugar ring structure on the C<sub>1</sub>–O–C<sub>5</sub> bond and sugar chain structure at the  $\beta$ -1,4 linkage. The increased aliphatic carbon may originate from the sugar condensation products, e.g., the brown solid. In all, these NMR

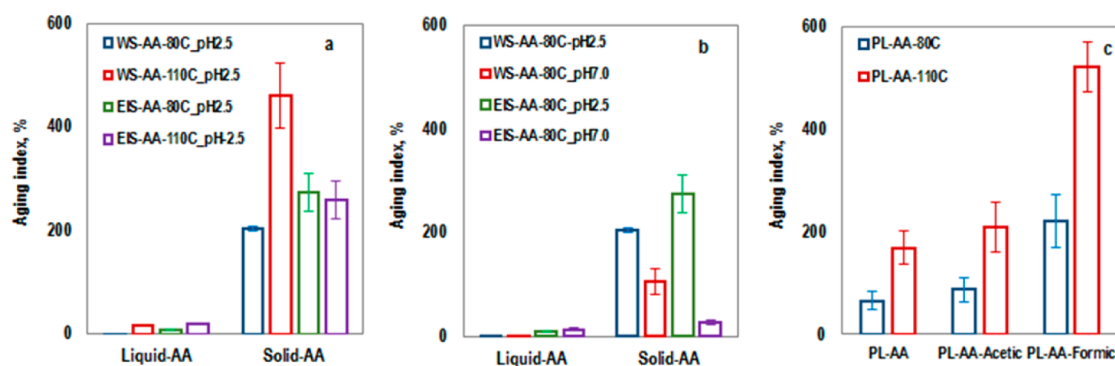


**Figure 2.** Mw aging index of bio-oil fractions after the accelerated aging test. (a) Aging indexes were obtained with WS (water soluble) and EIS (ether insoluble) fractions heated under pH 2.5 at 80 and 110 °C. (b) Aging indexes were obtained with WS and EIS fractions heated under pH 2.5 and 7.0 at 80 °C. (c) Aging indexes were obtained with WIS (water insoluble) lignin fraction with or without acid catalysts at 80 and 110 °C.

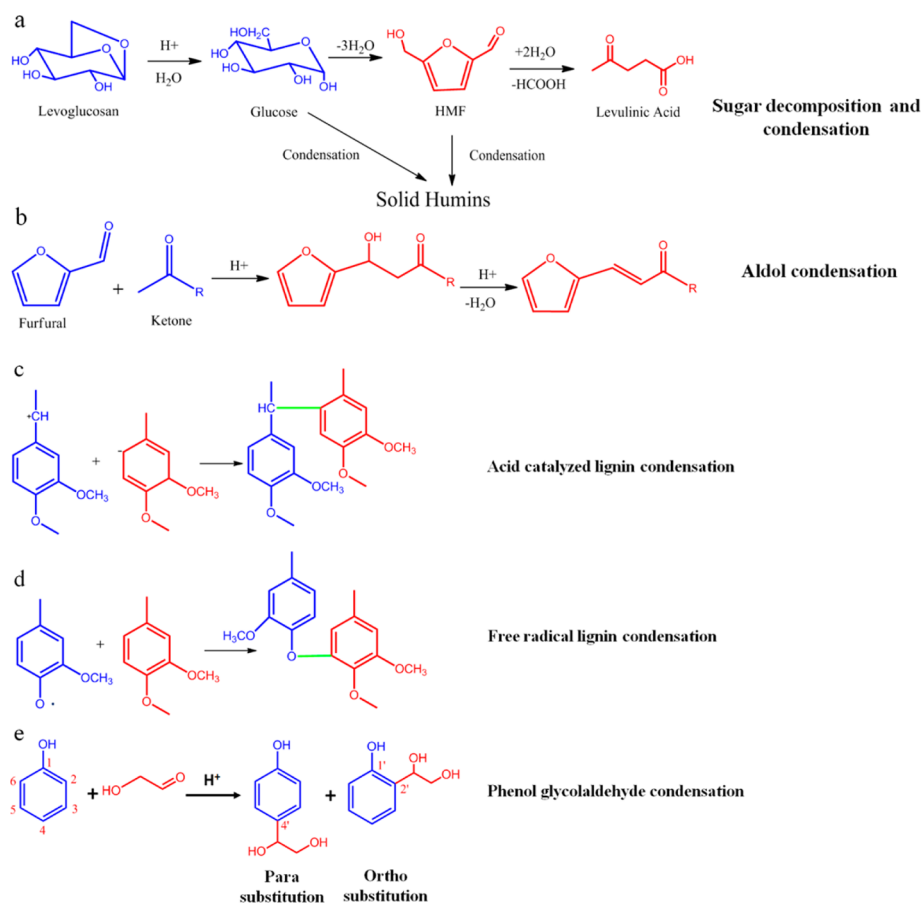


**Figure 3.** Tentative condensation of sugar and lignin fractions during bio-oil aging: (a) sugar decomposition and condensation forming humins, (b) aldol condensation of furfural and ketone, (c) acid-catalyzed lignin condensation, (d) radical initiated lignin condensation, and (e) phenol glycolaldehyde coupling. Aromatic carbon showed as  $C_1'$ ,  $C_2'$ , and  $C_4'$  after glycolaldehyde substitution.

**Table 2.**  $^{13}\text{C}$  NMR Characterization of Aged Pyrolytic Sugar<sup>a</sup> (EIS)

	210–166 ppm of carbonyl	166–110 ppm C=C	100–105 ppm of $C_1\text{--O--}C_4$	88–100 ppm of $C_1$ end	88–60 ppm of $C_{2,3,4,5,6}$	38–0 ppm aliphatic
EIS-Raw, %	6.8	4.7	11.5	20.0	45.8	11.2
EIS-AA <sup>b</sup> , %	4.9	8.1	10.6	16.7	45.7	14.0

<sup>a</sup>Integration range was determined based on carbon chemical shifts of a cellobiose model, and raw spectra can be found in Figure S1 of the Supporting Information. <sup>b</sup>Aging condition at 80 °C for 24 h.

**Table 3.**  $^{13}\text{C}$  NMR Characterization of Aged Pyrolytic Lignin (PL)<sup>a</sup>

	PL-Raw	PL-AA <sup>b</sup>	PL-AA acetic <sup>c</sup>	PL-AA formic <sup>d</sup>
210–166 ppm, carbonyl	3.7	5.8	6.2	6.9
166–142 ppm, aromatic C–O	15.1	20.4	20.2	23.6
142–125 ppm, aromatic C–C	22.6	25.0	23.9	27.2
125–102 ppm, aromatic C–H	25	22.4	21.6	17.8
90–58 ppm, aliphatic C–O	6.6	1.6	1.5	1.7
58–54 ppm, methoxyl/hydroxyl	2.4	2.1	2.3	1.3
37–10 ppm, aliphatic side chain	24.5	23.1	24.4	21.5

<sup>a</sup>Raw spectra can be found in Figure S2 of the Supporting Information. <sup>b</sup>Aging without acid catalyst. <sup>c</sup>Aging with adding an equal amount of acetic acid to pyrolytic lignin. <sup>d</sup>Aging with adding an equal amount of formic acid to pyrolytic lignin.

results support the two-stage sugar degradation and repolymerization mechanism.

**Accelerated Aging of Pyrolytic Lignin Fraction.** Phase separation and sticky gum (viscous liquid) formation are often observed after bio-oil aging especially at a high heating temperature. As the WS and EIS fractions did not produce such gum after aging, it is considered that these gum aggregates

are mainly formed from the condensation and aggregation of the bio-oil lignin fraction.

The average molecular weight of aged PL with/without acid addition is presented in Table S2 of the Supporting Information. As shown in Figure 2c, the molecular weight of aged PL increased significantly in an acid-free environment. Adding acetic acid could further promote the lignin

condensation; however, a more pronounced effect was not seen until formic acid was added. In addition, the increment was higher when the aging temperature was raised to 110 °C. It is well known that acid-catalyzed lignin condensation could take place between the electron-rich aromatic ring and the cationic site from benzyl alcohol and benzyl ether at the  $\alpha$ -carbon.<sup>21</sup> Such condensation will increase the amount of aromatic C–C linkage in the condensed lignin structure. Interestingly, PL also polymerized under an acid-free condition, which might be explained by a free radical reaction mechanism. As suggested by Britt and Kibert,<sup>22,23</sup> free radicals are generated during lignin pyrolysis, and the presence of these radicals in nature and kraft lignin has been reported.<sup>24</sup> Depending on the location of the radicals, the condensed lignin structure by radical reactions could feature an increased amount of aromatic C–O and C–C bonds.

The <sup>13</sup>C NMR analysis of the aged lignin is summarized in Table 3. These results of the aromatic carbon distribution support the above inference as the content of aromatic C–O and C–C bonds increased after aging, compared to that of the starting lignin. On the contrary, the aromatic C–H bond decreased. The aged lignin with acetic acid showed less significant change, compared to that with formic acid, suggesting the latter is more effective on lignin cross-linking. The carbon signals at 54–58 ppm that are often assigned to methoxy groups also decreased after aging. It was suggested that lignin demethoxylation can happen during the aging process.<sup>25</sup> However, methoxy groups may not be easily cleaved from aromatic ring unless strong acid or high temperature is employed. Under mild aging conditions in this study, the demethoxylation is less likely to happen, and this signal decrease might be associated with the reduction of other overlapped signals, e.g., the hydroxyl group attached to the  $\beta$ -carbon in the lignin side chain.

**Pyrolytic Lignin–Aldehyde Reaction.** In addition to the separate aging reactions within individual bio-oil fractions, mutual aging reactions may also exist. One of the most important interactions involves the condensation between phenolic compounds in the WIS fraction and aldehydes in the ES fraction through the well-known phenol–formaldehyde reaction.

**Model Compounds Study of Phenol–Glycolaldehyde Reaction.** GC/MS characterization on bio-oil made from loblolly pine identified glycolaldehyde as the most abundant aldehyde, and the content of this bifunctional chemical decreased by a factor of 2 after the aging. It may react with the PL and cause gum formation in the aged bio-oil. However, no reference has been found on reporting phenol–glycolaldehyde condensation. In order to verify the potential reaction between them, glycolaldehyde and phenol (1:1 by mole) were reacted with three different acid catalysts (acetic acid, formic acid, and HCl).

Acetic acid may have the least ability to catalyze the phenol–glycolaldehyde reaction as the liquid product only showed a slight color change after 24 h at 90 °C (Figure 4a). However, a black liquid solution after 12 h of heating was formed when formic acid was used (Figure 4b), and a free-flowing dark oil phase was formed in the vial containing HCl after 5 h (Figure 4c). As a control, the glycolaldehyde was also heated without adding phenol under an acidic condition (HCl, Figure 4d) for 2 h, and there was a significant amount of brown solids formed, suggesting that glycolaldehyde can undergo self-polymerization

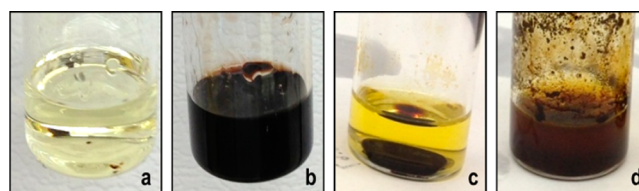


**Figure 4.** Phenol–glycolaldehyde reaction solutions with three different acid catalysts: (a) phenol–glycolaldehyde reaction with acetic acid, 24 h heating at 90 °C; (b) phenol–glycolaldehyde reaction with formic acid, 12 h heating at 90 °C; (c) phenol–glycolaldehyde reaction with HCl, 5 h heating at 90 °C; and (d) glycolaldehyde reaction formed with HCl without addition of phenol, 2 h heating at 90 °C.

via a direct condensation pathway similar to that shown in Figure 3a and b.

<sup>13</sup>C NMR analysis was performed, expecting that if the condensation between glycolaldehyde and phenol did occur, a similar reaction pathway that generates phenol–formaldehyde resin may be applied. Specifically, the reaction would start with aromatic electrophilic substitution (ortho or para) followed by a condensation step leading to cross-linking. However, compared to formaldehyde, glycolaldehyde has a bulky group (–CH<sub>2</sub>OH) attached to its aldehyde group, which may have a steric hindrance for the cross-linking reactions to take place, and it also has high tendency toward self-polymerization. Therefore, the condensation, if it exists, may only occur at a limited extent, i.e., dimerization. In addition, due to the dual functionality of glycolaldehyde (aldehyde and alcohol), various side-reactions could occur between glycolaldehyde and carboxylic acid catalysts.

As indicated in Figure 5, all the reaction products contained a significantly high amount of residual phenol, suggesting its low reactivity toward glycolaldehyde. The NMR spectrum of the oil phase (Figure 5c) from the hydrochloric acid-catalyzed reaction have a featured C<sub>1</sub> and C<sub>4</sub> aromatic substitution pattern. After ortho substitution, the aromatic C<sub>1</sub> shifted from 157.5 to 155.6 ppm (C<sub>1</sub>'), and C<sub>2</sub> shifted from 115.5 to 127.2 ppm (C<sub>2</sub>'). For the para substitution, the aromatic C<sub>4</sub> carbon shifted from 119.0 to 133.4 ppm (C<sub>4</sub>'), and a similar C<sub>1</sub> carbon shift was also observed. These chemical shifting patterns were confirmed with carbon-shift predications on the proposed substitution structures using ACD/NMR Processor 10.0, and satisfactory matching was obtained within ~0.3 ppm error. When formic acid was applied as the reaction catalyst, a similar ortho and para aromatic substitution can also be observed (Figure 5b) as C<sub>1</sub> shifted to C<sub>1</sub>' from 157.2 to 155.8 ppm, C<sub>2</sub> shifted to C<sub>2</sub>' from 115.2 to 127.4 ppm, and C<sub>4</sub> shifted to C<sub>4</sub>' from 118.8 to 132.0 ppm. For acetic acid (Figure 5a), however, such a substitution pattern has not been detected indicating no reaction between phenol and glycolaldehyde in a weak acid reaction medium.

In addition to the aromatic carbons discussed above, the NMR spectra for the phenol–glycolaldehyde reaction with acetic acid and formic acid (Figure 5a and b) were found to be more complicated than that with HCl (Figure 5c). A strong signal assigned to a carbonyl ester carbon (~163 ppm) can be identified for the formic acid-catalyzed reaction indicating the esterification between formic acid and glycolaldehyde. Acetic acid can also react with glycolaldehyde forming acetyloxyacetaldehyde. In Figure 5a and b, the weak carbonyl carbon (aldehyde type) signal at 200–210 ppm indicates the presence

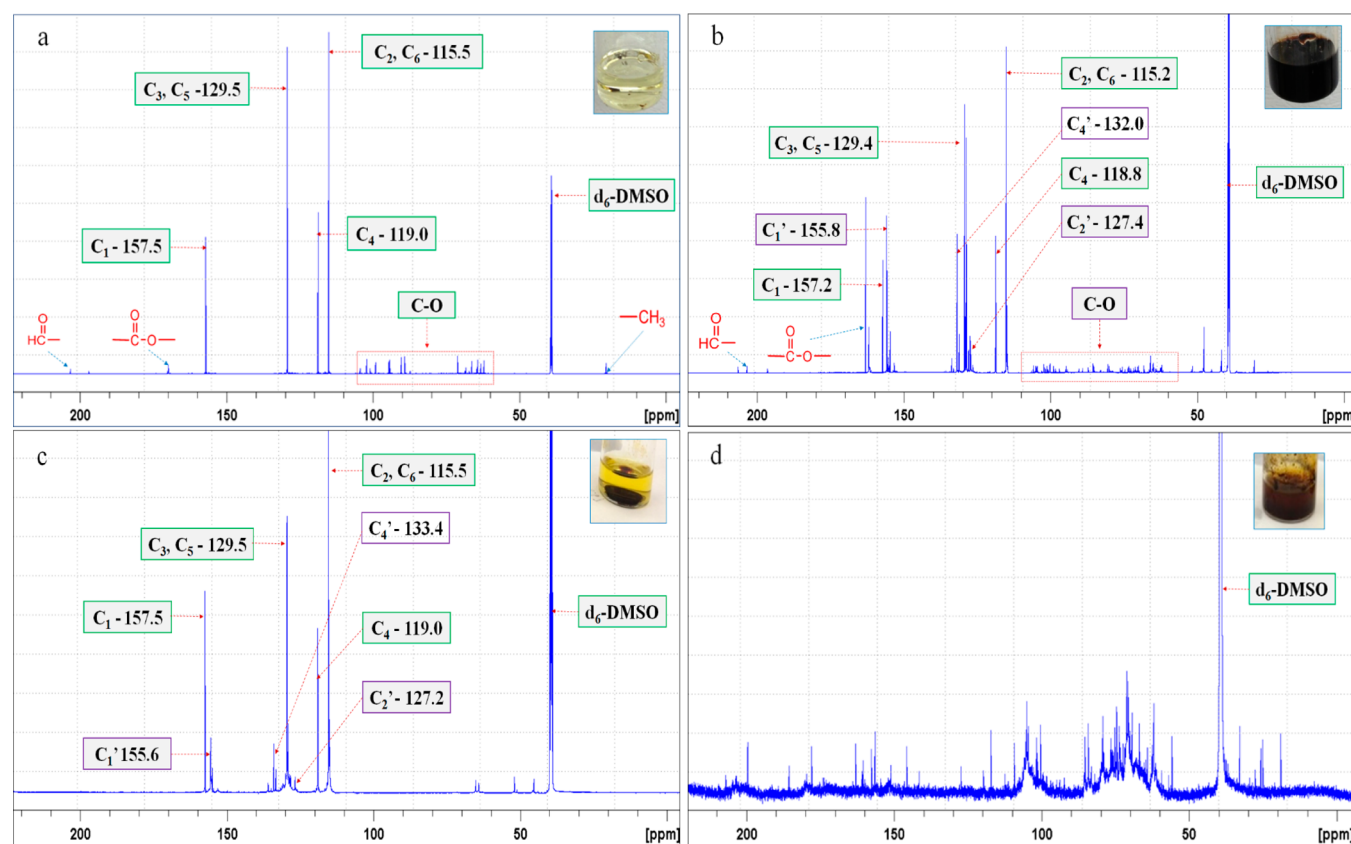


**Figure 5.**  $^{13}\text{C}$  NMR characterization of phenol–glycolaldehyde reaction products: (a) phenol–glycolaldehyde reaction product formed with acetic acid, (b) phenol–glycolaldehyde reaction product formed with formic acid, (c) phenol–glycolaldehyde reaction product formed with HCl, and (d) glycolaldehyde reaction control without addition of phenol formed with HCl acid.

of a residual aldehyde in the final reaction product. In addition, a series of oxygen-attached carbon signals were also found between 60 and 110 ppm, which may originate from the hydroxyl carbons in the self-polymerized glycolaldehyde polymers as similar carbon signals (Figure 4d) were also detected in the control reaction.

**Accelerated Aging of Pyrolytic Lignin with Aldehydes under Acidic Conditions.** Formaldehyde, furfural, and HMF are well-known aldehydes that could react with phenol to produce phenolic resins.<sup>26</sup> Glycolaldehyde, as discussed above, also has limited reactivity with phenol. To test the potential condensation between aldehydes and PL, five different aldehydes previously identified in bio-oil (formaldehyde, glycolaldehyde, furfural, HMF, and vanillin) were reacted with PL at accelerated aging conditions. Acetic acid ( $\text{p}K_{\text{a}} = 4.75$ ) and formic acid ( $\text{p}K_{\text{a}} = 3.75$ ), commonly found in the bio-oil, were able to completely dissolve PL and were used as reaction catalysts. Mineral acids were intentionally excluded here as their presence in bio-oil was not confirmed. Two PL controls (without adding aldehydes) dissolved in acetic acid or formic acid were also included.

Before the reaction, the lignin–aldehyde mixtures were well dissolved in acid as a uniform liquid solution. After heating under an acetic acid condition, the lignin–formaldehyde solution turned into a solid, but other samples were still in a viscous liquid form. In the case of formic acid, black solid chunks were formed after aging, suggesting a higher degree of lignin condensation. Moreover, the aged lignin–formaldehyde products (formic acid catalyst) cannot fully dissolve in THF

indicating a resin formation; therefore, only the THF soluble fraction was characterized with GPC and  $^{13}\text{C}$  NMR.

The average Mw of lignin–aldehyde products are summarized in Table S3 of the Supporting Information, and its Mw aging index comparisons are expressed in Figure 6. For the lignin–aldehyde reaction in an acetic acid solution, only formaldehyde significantly cross-linked the lignin units as the aging index is 690%. A  $^{13}\text{C}$  NMR characterization of this condensed lignin also showed a strong methylene bridge at  $\sim 30$

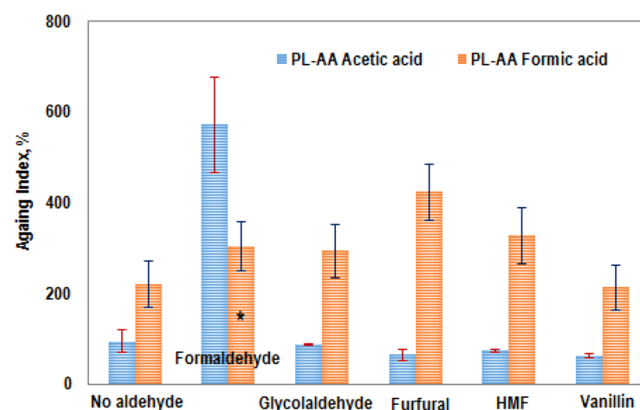


**Figure 6.** Mw aging index of the pyrolytic lignin–aldehydes reaction products with different acid catalysts. Asterisk (\*) indicates that the value was calculated based on the THF soluble portion of the aged PL (pyrolytic lignin) with formaldehyde and formic acid due to its insoluble resin product.

ppm<sup>27</sup> indicating an ortho–ortho or ortho–para linkage between the two phenolic units connected by substituted formaldehyde. Other aldehydes, including glycolaldehyde, furfural, HMF, and vanillin, did not show such an effect. Particularly, the glycolaldehyde cannot effectively condense the lignin model compound (phenol in acetic acid) as investigated above.

On the contrary, when formic acid was used to catalyze the lignin–aldehyde reaction, most of the aldehydes used in this study seem to promote the condensation, except that vanillin showed no reactivity as the Mw was almost identical to that of the control (no aldehyde). NMR characterization on the phenol–vanillin reaction product showed a fringe-printed vanillin carbon signal indicating that it did not participate in the coupling reaction. Among other active aldehydes, formaldehyde showed the highest reactivity toward PL cross-linking due to the formation of THF insoluble resin. Strong chemical linkage between phenol and formaldehyde observed in <sup>13</sup>C NMR further confirm the reaction. Although aged PL with glycolaldehyde, furfural, and HMF addition also showed higher Mw than that of the control PL, no solid resins were obtained indicating their low reactivity toward lignin condensation. Moreover, the <sup>13</sup>C NMR characterization of these reacted lignin samples showed a featured glycolaldehyde self-condensation pattern similar to that shown in Figure Sd and an excessive amount of residual furfural and HMF. More importantly, no strong evidence has been found in their NMR spectra suggesting that they have been coupled with phenol. This explains why formaldehyde reacts faster than glycolaldehyde, HMF, furfural with phenol, and it also indicates that they did not effectively promote the lignin condensation. The increased Mw may be largely due to aldehyde self-condensation or other side condensation reactions, e.g., esterification with acid catalyst.

**Proposed Bio-Oil Aging Pattern.** On the basis of these observations, a conceptual model of bio-oil aging is proposed. The bio-oil is composed of the WS fraction (ES and EIS fractions) and the WIS fraction (PL). Each of these fractions undergo different aging reactions forming aged bio-oil. The WIS fraction condensed after aging, and as a result, it may separate itself from the bio-oil microstructure to form sticky gum aggregates. The WS fraction and its subfraction, namely, EIS (pyrolytic sugar), formed brown solids after aging. The sugar fraction may decompose into aldehydes and acids and then repolymerize through an unidentified reaction pathway forming humins. The ES fraction was not directly aged in this study. However, its high reactivity can be measured as it contains highly reactive components; esterification, acetalization, and/or aldol-condensation could occur in this fraction.

In addition, each bio-oil fraction could have a synergistic effect on promoting the bio-oil condensation degree. For example, the acids in the ES and WS fractions could promote the condensation of the lignin fraction and decomposition of the sugar fraction. Aldehydes, especially formaldehyde in the ES fraction, could effectively cross-link PL even with weak acetic acid. It appears that these mutual interactions are critical reasons for bio-oil aging. If acids could be removed from the WS fraction, then acid condensation of lignin and lignin–aldehyde reactions would not take place and sticky gum aggregates may not be formed. The proposed pattern could serve as grounds to further develop and understand the bio-oil aging mechanism.

## CONCLUSIONS

A high degree of condensation measured by average molecular weight was found with an increase in aging temperature and the presence of acids in fractionated bio-oils. It was also observed that solid residue was generated when water soluble and ether insoluble fractions from pyrolysis bio-oil were aged. The aging index of the solids fraction increased 2-fold for the WS fraction at the aging temperature of 110 °C compared to 80 °C, while it decreased by 10 times for the EIS fraction when the pH was adjusted from 2.5 to 7.0 at the aging temperature of 80 °C. A similar trend was found for the lignin fraction, and formic acid can significantly increase the degree of condensation: 220% vs a 64% and 87% increase in an acid-free and acetic acid environment, respectively. A model compounds study was conducted to understand the phenol–glycolaldehyde reaction, and it was found that the glycolaldehyde can react with phenol but to a limited extent (dimerization) in the presence of a proper acid catalyst (e.g., HCl and formic acid). Various aldehydes identified in bio-oil such as formaldehyde can increase the molecular weight of aged pyrolytic lignin, while only formaldehyde showed evidence of chemical cross-linking the lignin units. The molecular weight of the lignin–formaldehyde complex increased 4 times with acetic acid compared to that without formaldehyde addition, while it is beyond measurement in formic acid solution due to the resin formation. The results presented in this study suggest that a bio-oil aging model can be constructed within or between bio-oil fractions.

## ASSOCIATED CONTENT

### Supporting Information

Tables S1, S2, and S3 and Figures S1 and S2 regarding the average molecular weight data and <sup>13</sup>C NMR characterization spectra of the ether insoluble fraction and pyrolytic lignin. This material is available free of charge via the Internet at <http://pubs.acs.org>.

## AUTHOR INFORMATION

### Corresponding Author

\*Phone: +1 919-515-0473. Fax: +1 919-515-6302. E-mail: [sunkyu\\_park@ncsu.edu](mailto:sunkyu_park@ncsu.edu).

### Present Address

J. Meng: Environment and Energy Center, Southern Research Institute, 5201 International Dr., Durham, North Carolina 27712, United States.

### Author Contributions

The manuscript was written through contributions of all authors. All authors have given approval to the final version of the manuscript. All authors contributed equally.

### Notes

The authors declare no competing financial interest.

## ACKNOWLEDGMENTS

The authors thank Dr. David Dayton and Dr. John Carpenter at RTI International for the help with measuring bio-oil TAN number. This IBSS project is supported by the Agriculture and Food Research Initiative Competitive Grant 2011-68005-30410 from the USDA National Institute of Food and Agriculture.

## ■ ABBREVIATIONS

PL, pyrolytic lignin; WS, water soluble; WIS, water insoluble; ES, ether soluble; EIS, ether insoluble

## ■ REFERENCES

- (1) Bertero, M.; de la Puente, G.; Sedran, U. Effect of pyrolysis temperature and thermal conditioning on the coke-forming potential of bio-oils. *Energy Fuels* **2011**, *25* (3), 1267–1275.
- (2) Naske, C. D.; Polk, P.; Wynne, P. Z.; Speed, J.; Holmes, W. E.; Walters, K. B. Postcondensation filtration of pine and cottonwood pyrolysis oil and impacts on accelerated aging reactions. *Energy Fuels* **2011**, *26* (2), 1284–1297.
- (3) Baldwin, R. M.; Feik, C. J. Bio-oil stabilization and upgrading by hot gas filtration. *Energy Fuels* **2013**, *27* (6), 3224–3238.
- (4) Diebold, J. P. A Review of the Chemical and Physical Mechanisms of the Storage Stability of Fast Pyrolysis Bio-Oils. In *Fast Pyrolysis of Biomass: A Handbook*; Bridgwater, A. V., Ed.; CPL Press: Newbury, U.K., 2002; pp 205–241.
- (5) Diebold, J. P.; Czernik, S. Additives to lower and stabilize the viscosity of pyrolysis oils during storage. *Energy Fuels* **1997**, *11* (5), 1081–1091.
- (6) Xu, F.; Xu, Y.; Lu, R.; Sheng, G.-P.; Yu, H.-Q. Elucidation of the thermal deterioration mechanism of bio-oil pyrolyzed from rice husk using fourier transform infrared spectroscopy. *J. Agric. Food Chem.* **2011**, *59* (17), 9243–9249.
- (7) He, R.; Ye, X. P.; Harte, F.; English, B. Effects of high-pressure homogenization on physicochemical properties and storage stability of switchgrass bio-oil. *Fuel Process. Technol.* **2009**, *90* (3), 415–421.
- (8) Chaala, A.; Ba, T.; Garcia-Perez, M.; Roy, C. Colloidal properties of bio-oils obtained by vacuum pyrolysis of softwood bark: Aging and thermal stability. *Energy Fuels* **2004**, *18* (5), 1535–1542.
- (9) Hu, X.; Wang, Y.; Mourant, D.; Gunawan, R.; Lievens, C.; Chaiwat, W.; Gholizadeh, M.; Wu, L.; Li, X.; Li, C.-Z. Polymerization on heating up of bio-oil: A model compound study. *AIChE J.* **2013**, *59* (3), 888–900.
- (10) Fratini, E.; Bonini, M.; Oasmaa, A.; Solantausta, Y.; Teixeira, J.; Baglioni, P. SANS analysis of the microstructural evolution during the aging of pyrolysis oils from biomass. *Langmuir* **2005**, *22* (1), 306–312.
- (11) Oasmaa, A.; Kuoppala, E.; Solantausta, Y. Fast pyrolysis of forestry residue. 2. Physicochemical composition of product liquid. *Energy Fuels* **2003**, *17*, 433–443.
- (12) Meng, J.; Park, J.; Tilotta, D.; Park, S. The effect of torrefaction on the chemistry of fast-pyrolysis bio-oil. *Bioresour. Technol.* **2012**, *111* (0), 439–446.
- (13) Oasmaa, A.; Meier, D. Norms and standards for fast pyrolysis liquids: 1. Round robin test. *J. Anal. Appl. Pyrolysis* **2005**, *73* (2), 323–334.
- (14) Elliott, D. C.; Oasmaa, A.; Preto, F.; Meier, D.; Bridgwater, A. V. Results of the IEA round robin on viscosity and stability of fast pyrolysis bio-oils. *Energy Fuels* **2012**, *26* (6), 3769–3776.
- (15) Yaylayan, V. A.; Harty-Majors, S.; Ismail, A. A. Investigation of the mechanism of dissociation of glycolaldehyde dimer (2,5-dihydroxy-1,4-dioxane) by FTIR spectroscopy. *Carbohydr. Res.* **1998**, *309* (1), 31–38.
- (16) Scholze, B.; Hanser, C.; Meier, D. Characterization of the water-insoluble fraction from fast pyrolysis liquids (pyrolytic lignin): Part II. GPC, carbonyl groups, and  $^{13}\text{C}$ -NMR. *J. Anal. Appl. Pyrolysis* **2001**, *58*–*59* (0), 387–400.
- (17) Tessini, C.; Müller, N.; Mardones, C.; Meier, D.; Berg, A.; von Baer, D. Chromatographic approaches for determination of low-molecular mass aldehydes in bio-oil. *J. Chromatogr. A* **2012**, *1219* (0), 154–160.
- (18) Wildschut, J.; Mahfud, F. H.; Venderbosch, R. H.; Heeres, H. J. Hydrotreatment of fast pyrolysis oil using heterogeneous noble-metal catalysts. *Ind. Eng. Chem. Res.* **2009**, *48* (23), 10324–10334.
- (19) Gayubo, A. G.; Valle, B.; Aguayo, A. T.; Olazar, M.; Bilbao, J. Pyrolytic lignin removal for the valorization of biomass pyrolysis crude bio-oil by catalytic transformation. *J. Chem. Technol. Biotechnol.* **2010**, *85* (1), 132–144.
- (20) Lu, Q.; Zhang, Y.; Tang, Z.; Li, W.-z.; Zhu, X.-f. Catalytic upgrading of biomass fast pyrolysis vapors with titania and zirconia/titania based catalysts. *Fuel* **2010**, *89* (8), 2096–2103.
- (21) Shimada, K.; Hosoya, S.; Ikeda, T. Condensation reactions of softwood and hardwood lignin model compounds under organic acid cooking conditions. *J. Wood Chem. Technol.* **1997**, *17* (1–2), 57–72.
- (22) Britt, P. F.; Buchanan Iii, A. C.; Thomas, K. B.; Lee, S.-K. Pyrolysis mechanisms of lignin: Surface-immobilized model compound investigation of acid-catalyzed and free-radical reaction pathways. *J. Anal. Appl. Pyrolysis* **1995**, *33* (0), 1–19.
- (23) Kibet, J.; Khachatryan, L.; Dellinger, B. Molecular products and radicals from pyrolysis of lignin. *Environ. Sci. Technol.* **2012**, *46* (23), 12994–13001.
- (24) Steelink, C. Stable Free Radicals in Lignin and Lignin Oxidation Products. In *Lignin Structure and Reactions*; Marton, J., Ed.; Advances in Chemistry Series 59; American Chemical Society: Washington, DC, 1966; pp 51–64.
- (25) Ben, H.; Ragauskas, A. J. In situ NMR characterization of pyrolysis oil during accelerated aging. *ChemSusChem* **2012**, *5* (9), 1687–1693.
- (26) Knop, A.; Pilato, L. A. Phenolic Resins Chemistry. In *Applications and Performance Future Directions*; Springer-Verlag: Berlin, 1985.
- (27) Werstler, D. D. Quantitative  $^{13}\text{C}$  n.m.r. characterization of aqueous formaldehyde resins: 1. Phenol-formaldehyde resins. *Polymer* **1986**, *27* (5), 750–756.